

Visualization of transcatheter ablation of septal hypertrophy in patients with hypertrophic obstructive cardiomyopathy: a comparison between cardiac MRI, invasive measurements and echocardiography

Christian Sohns · Samuel Sossalla · Jan D. Schmitto · Claudius Jacobshagen · Björn W. Raab · Silvia Obenauer · Lars S. Maier

Received: 1 November 2009 / Accepted: 22 January 2010 / Published online: 21 February 2010
© The Author(s) 2010. This article is published with open access at Springerlink.com

Abstract

Objective Hypertrophic obstructive cardiomyopathy (HOCM) is treated by surgical myectomy or transcatheter ablation of septal hypertrophy (TASH). The aim of this study was to visualize the feasibility, success and short-term results of TASH on the basis of cardiac MRI (CMR) in comparison with cardiac catheterization and echocardiography.

Methods In this in vivo study, nine patients with HOCM were treated with TASH. Patients were evaluated by transthoracic echocardiography, invasive cardiac angiography and CMR. Follow-up examinations were carried out after 1, 3 and 12 months. MR imaging was performed on a 1.5-T scanner. All images were processed using the semi-automatic Argus software and were evaluated by an attending thoracic radiologist and cardiologist.

Results The echocardiographic pressure gradient (at rest) was 69.3 ± 15.3 mmHg before and 22.1 ± 5.7 mmHg after TASH ($P < 0.01$, $n = 9$). The flux acceleration over the aortic valve examined (V_{\max}) was 5.1 ± 0.6 m/s before and

3.4 ± 0.3 m/s after the TASH procedure ($P < 0.05$). Also, there was a decrease of septum thickness from 22.0 ± 1.2 to 20.2 ± 1.0 mm ($P < 0.05$) after 6 ± 3 weeks. The invasively assessed pressure gradient at rest was reduced from 63.7 ± 15.2 to 21.2 ± 11.1 mmHg ($P < 0.01$) and the post-extrasystolic gradient was reduced from 138.9 ± 12.7 to 45.6 ± 16.5 mmHg ($P < 0.01$). All differences as well as the quantity of injected ethanol were plotted against the size or amount of scar tissue as assessed in the MRI. There was a statistically significant correlation between the post-extrasystolic gradient decrease and the amount of scar tissue ($P = 0.03$, $r^2 = 0.5$). In addition, the correlation between the quantity of ethanol and scar tissue area was highly significant ($P < 0.01$, $r^2 = 0.6$), whereas the values for the gradient deviation ($P = 0.10$, $r^2 = 0.34$), ΔV_{\max} ($P = 0.12$, $r^2 = 0.31$), as well as the gradient at rest ($P = 0.27$, $r^2 = 0.17$) were not significant.

Conclusion TASH was consistently effective in reducing the gradient in all patients with HOCM. In contrast to the variables investigated by echocardiography, the invasively measured post-extrasystolic gradient correlated much better with the amount of scar tissue as assessed by CMR. We conclude that the optimal modality to visualize the TASH effect seems to be a combination of CMR and the invasive identification of the post-extrasystolic gradient.

Keywords HOCM · TASH · CMR · Cardiac imaging

S. Obenauer and L. S. Maier, contributed equally.

C. Sohns · S. Sossalla · J. D. Schmitto · C. Jacobshagen ·
B. W. Raab · S. Obenauer · L. S. Maier (✉)
Department of Cardiology and Pneumology/Heart Center,
Georg-August-University Goettingen, Robert-Koch-Str. 40,
37075 Goettingen, Germany
e-mail: lmaier@med.uni-goettingen.de

J. D. Schmitto
Division of Cardiac Surgery,
Brigham and Women's Hospital,
Harvard Medical School, Boston, USA

B. W. Raab · S. Obenauer
Department of Radiology,
Georg-August-University Goettingen, Goettingen, Germany

Abbreviations

HOCM Hypertrophic obstructive cardiomyopathy
TASH Transcatheter ablation of septal hypertrophy
CMR Cardiac MRI
LVOT Left ventricular outflow tract
 V_{\max} Flux acceleration over the aortic valve

RBBB	Right bundle branch block
LVEF	Left ventricular ejection fraction
CK	Creatine kinase
CAD	Coronary artery disease

Introduction

Hypertrophic obstructive cardiomyopathy (HOCM) is a relatively common genetic cardiovascular disease with a prevalence of $\sim 1:500$ [1]. Patients with HOCM often present with symptoms of heart failure and insufficient response to medical treatment [2–5]. The most frequent therapy applied to these patients is surgical myectomy (removing a small amount of myocardium from the basal interventricular septum) [6–9]. This substantially reduces the subaortic outflow gradient in more than 90% of patients and results in persistent symptomatic improvement in about 70–90% [2, 5, 7–10]. In the last few years, minimally invasive transcatheter ablation of septal hypertrophy (TASH) by selective transcatheter septal branch injection of ethanol has shown to reduce substantially outflow tract obstruction in 80–90% and reduction of symptoms in 84–90% of the treated patients [11–19]. Consequently, TASH may be an effective alternative to surgery [20–27]. To avoid collateral damage like right bundle branch block (RBBB) or high-grade atrioventricular block it is important to estimate the anatomical conditions before starting the intervention. Therefore, the purpose of the present study was to visualize the feasibility, hemodynamical success, and short term results of TASH on the basis of intracardiac catheterization, cardiac MRI (CMR), and echocardiography before and after the TASH procedure.

Materials and methods

To visualize the feasibility, hemodynamic success, and short term results of TASH intracardiac catheterization, CMR and echocardiography were conducted at baseline and in follow-up studies after 1, 3, and 12 months following the TASH procedure. All patients were monitored in the intensive or coronary care unit for at least 48 h. ECG and cardiac enzyme controls were assessed every 4 h until the CK peak was reached. Before discharge, noninvasive follow-up included Doppler assessments of the residual LVOT gradient.

Patient inclusion

TASH was applied to nine patients (median age 62 ± 6 years, six females and three males) with HOCM. The diagnosis of HOCM was based on the common clinical

Table 1 Clinical characteristics of nine patients undergoing catheter-based treatment for HOCM by TASH

Patient characteristics	
Total no. of patients	9
Male/female sex no.	3/6
Age (years)	62 ± 6
Septum thickness (mm)	22.0 ± 1.2
Echocardiographic pressure gradient (mmHg)	69.3 ± 15.3
Echocardiographic flux acceleration (V_{\max}) (m/s)	5.1 ± 0.6
Invasive gradient at rest (mmHg)	63.7 ± 15.2
Invasive postextrasystolic gradient (mmHg)	138.9 ± 12.7
Ethanol injection (ml)	1.8 ± 0.3

and two-dimensional echocardiographic criteria [1]. Obstruction was defined by an LVOT gradient under resting conditions and after provocation of at least 30 mmHg [1]. Detailed patients' characteristics are presented in the Table 1. A written informed consent was obtained from each patient.

Echocardiographic examination

Transthoracic and transesophageal echocardiography was performed on Philips Sonos 5500 (Philips Medical Systems) and recorded on an S-VHS video to allow serial review and side-by-side comparison of the studies. Standard probes were used for transthoracic and transesophageal echocardiography. Basal ventricular septal thickness was divided from an integrated analysis of M-mode and two-dimensional echocardiograms. The M-mode echocardiograms were derived from direct anatomical visualization of the two-dimensional images. All measurements were made according to the recommendations of the American Society of Echocardiography [28]. The two-dimensional echocardiographic images were obtained in the parasternal long- and short-axis views and apical two- and four-chamber views using standard transducer positions. For transesophageal acquisition, the probe was placed in the mid-esophageal position, where an adequate four-chamber view could be obtained. Short-axis views were derived from a basal gastric position. Care was taken to achieve a similar probe position for the follow-up examinations. Systolic anterior motion of the mitral valve was defined as mild, moderate or severe according to Gilbert et al. [29]. Echocardiographic examinations were conducted at baseline, 6 ± 3 weeks, 3 months, and 1 year after TASH.

TASH procedure

In each case, the gradient at rest and the post-extrasystolic gradient were measured before and after the procedure.

Briefly, a suitable proximal branch of the left anterior descending coronary artery was identified by a gradient-guided technique under programmed electrical stimulation. By using this technique, significantly smaller amounts of ethanol could be used by titrating the ethanol dose according to the angiographic washout velocity and real-time measured reduction of the intraventricular pressure gradient. Programmed electrical stimulation was used to provoke premature ventricular beats under reproducible conditions to assess post-extrasystolic potentiation of the gradient. Using this technique the fixed coupling interval is followed by an identical duration of the left ventricular filling period and a constant magnitude of the subsequently provoked gradient which correlates significantly with the gradient after physical exercise [23, 30]. Ethanol was injected only in case of a clear reduction of the gradient during testing the effect of a transient balloon occlusion of the septal vessel.

CMR investigation

CMR was carried out 10 ± 4 weeks after TASH. MR imaging was performed on a 1.5-T scanner (Magnetom; Siemens, Germany) with 40-mT/m maximum gradient strength and a phased array body coil. Investigation time was about 30–40 min. Patients were studied in a supine position with breath-holding-technique. Short-axis cine MRI of the entire left ventricle from the base to the apex was performed for the analysis of cardiac mass and function. Heart rate, vectorcardiogram and blood pressure were monitored.

The left ventricular function was assessed by a segmented two-dimensional electrocardiographically triggered fast low-angle shot-pulse sequence in the cine mode (TR 23.8 ms, TE 1.49 ms, flip angle 59° , basic resolution 256×256 , voxel size $2.0 \text{ mm} \times 1.6 \text{ mm} \times 5 \text{ mm}$, slice thickness 5 mm, chronological resolution 50 ms, field of view phase 81.3%, phase resolution 79%, distance factor 20% and field of view reading up to 500 mm). The number of cardiac phases imaged depended on the heart rate. Typically, 16 phases per cardiac cycle were obtained. Three short-axis planes were obtained; slice positions were taken from the cine MR imaging data set. The basal slice was the first to show circumferential myocardium at both diastole and systole. The apical slice was the last to show the intracavity blood pool in all phases over the cardiac cycle. The mid-ventricular slice was positioned halfway between the basal slice and the apical slice.

The left ventricular ejection fraction (LVEF) was estimated from the short-axis planes. Therefore, a segmented two-dimensional electrocardiographically triggered fast low-angle shot-pulse sequence was used during breath-holding (TR 23.8 ms, TE 1.49 ms, flip angle 59° , basic resolution 256×256 , voxel size $2.0 \text{ mm} \times 1.6 \text{ mm} \times 5 \text{ mm}$, slice thickness 5 mm, chronological resolution

50 ms, field of view phase 81.3%, phase resolution 79%, distance factor 20% and field of view reading up to 500 mm). The number of cardiac phases imaged depended on the heart rate.

Image analysis

Tagged images were processed using the semiautomatic ARGUS software (version 2004 A; Siemens, Germany) and were evaluated by an attending thoracic radiologist and cardiologist. The area of interest was the ventricular septum and the subaortic region. The endo- and epicardial contours were defined in the end-diastolic frame and the software then detected the tag grid using an affine plus anisotropic radial scaling transform algorithm. The grid was adapted to each of the acquired images from the end-diastolic to the end-systolic frame, mass, left and right ventricular ejection fraction. If necessary, manual correction was performed by moving, adding, or deleting tag intersections. Evaluation time for tracking the tag intersections of one slice was about 30 min.

Left ventricular function and mass was also analyzed. After the determination of the end-diastolic and end-systolic frame on the first basal slice to show circumferential myocardium at both diastole and systole, the endocardial and epicardial contours were traced manually by two investigators. The papillary muscles were included in the measured ventricular volume. To account for body height and mass, indexes were calculated related to 1 m^2 of body surface area for volumes and masses. Parameters of global function of the left ventricle were end-diastolic and end-systolic volume index and ejection fraction. The ventricular mass index was obtained by the multiplication of the mean wall volume of the end-diastolic and the end-systolic frames and the specific weight of cardiac muscle (1.05 g/mL). All volumes were calculated automatically by summing the areas in the entire series of short-axis cine images.

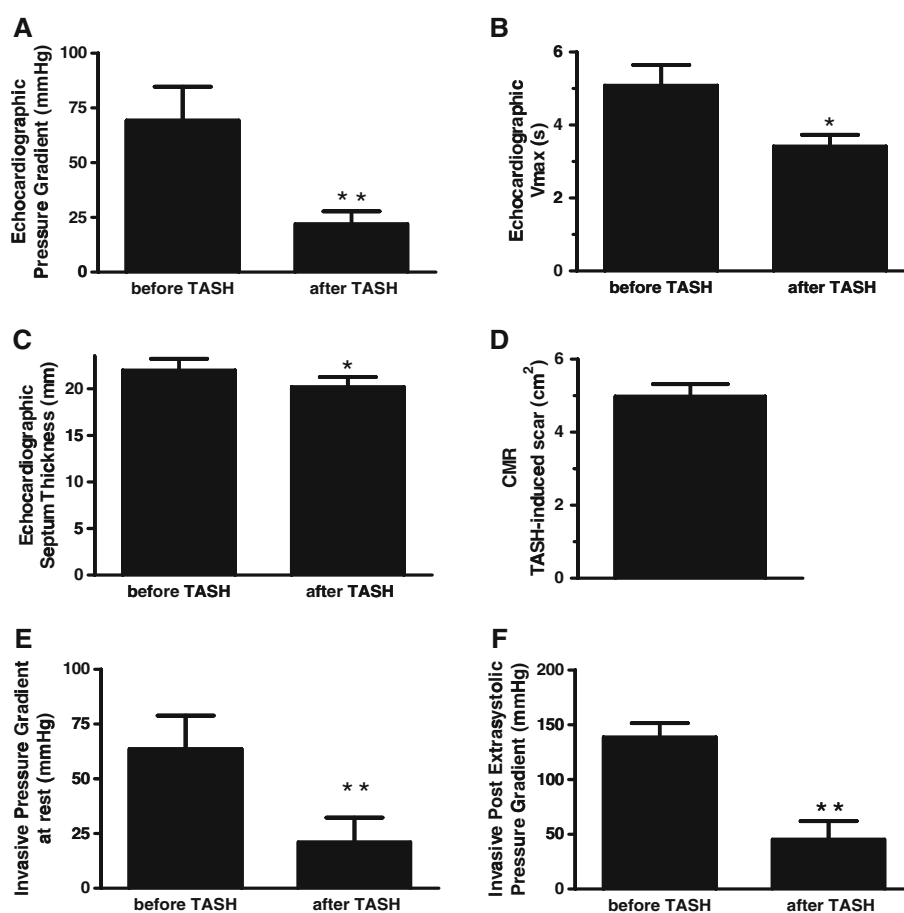
Data analysis and statistics

All data are expressed as mean \pm SEM. Student's paired *t* test was used to test for significance. $P < 0.05$ was considered significant. A linear regression analysis was used for comparing gradient data and ethanol injection with myocardial scar tissue. GraphPad Prism 5 was used to perform the regression analysis and Microsoft Excel was used in the case of paired *t* test of normal distributed data.

Results

TASH was highly effective in improving hemodynamic and anatomic conditions. Figure 1 shows the differences in

Fig. 1 Effectiveness of the TASH procedure. **a** Echocardiographic examination of the LVOT gradient at rest, **b** the flux acceleration (V_{\max}) over the aortic valve and **c** septum thickness before and after TASH. **d** Broadening of scar tissue by CMR. Invasive cardiac catheter examination of **e** the basal pressure gradient and **f** the post-extrasystolic gradient before and after TASH. * $P < 0.05$, ** $P < 0.01$ versus before TASH, respectively



LVOT gradient, flux acceleration (V_{\max}), septum thickness, pressure gradient at rest, post-extrasystolic gradient before and after TASH, as well as the corresponding scar tissue.

The echocardiographic pressure gradient could be significantly reduced by the TASH intervention. The LVOT gradient was reduced from 69.3 ± 15.3 to 22.1 ± 5.7 mmHg (Fig. 1a, $n = 9$ patients each, $P < 0.01$). Moreover, V_{\max} was decreased from 5.1 ± 0.6 to 3.4 ± 0.3 m/s (Fig. 1b, $P < 0.05$). There was a decrease of septum thickness from 22.0 ± 1.2 to 20.2 ± 1.0 mm (Fig. 1, $P < 0.05$).

After the successful TASH procedure the scar tissue was appraised by CMR. The mean scar tissue area was $5.0 \pm 0.3 \text{ cm}^2$ (Fig. 1d). The intracardiac catheter delivers the corresponding gradients in situ. The invasively assessed LVOT pressure gradient at rest was decreased from 63.7 ± 15.2 to 21.2 ± 11.1 mmHg (Fig. 1e, $P < 0.01$), and the post-extrasystolic gradient was reduced from 138.9 ± 12.7 to 45.6 ± 16.5 mmHg (Fig. 1f, $P < 0.01$).

To further visualize the operability and success of TASH the echocardiographic and invasive measurements were correlated with the accordant CMR scar tissue area into the ventricular septum in the subaortic region. Figure 2 demonstrates the correlation between the scar size and the

echocardiographically and invasively assessed parameters. Figure 2d demonstrates a significant correlation between the scar size and the invasively measured post-extrasystolic gradient reduction ($P < 0.05$, $r^2 = 0.5$), whereas the values for the echocardiographic gradient deviation (Fig. 2a, $P = 0.10$, $r^2 = 0.34$), ΔV_{\max} (Fig. 2b, $P = 0.12$, $r^2 = 0.31$), as well as the invasive gradient at rest (Fig. 2c, $P = 0.27$, $r^2 = 0.17$) were not significant. To evaluate the different effects of varying ethanol dosing within the procedure, the CMR scar tissue area was correlated with the quantity of injected ethanol. Our data showed a significant correlation between the amount of ethanol and the scar tissue (Fig. 3, $P < 0.01$, $r^2 = 0.6$).

Discussion

In 1995, Sigwart et al. [12] were the first to describe the effect of occluding a septal perforator artery with ethanol on the pressure gradient in HOCM. This procedure provoked a localized septal infarction and was referred to as nonsurgical septal reduction therapy (NSRT). Subsequently, two German centers reported extensive experience with many hundreds of patients [13, 31]. Seggewiss et al. [31] have

Fig. 2 Correlation between effectiveness of TASH and scar tissue. **a** Echocardiographic LVOT gradient deviation at rest, **b** flux acceleration reduction (ΔV_{max}), **c** Decrease of the angiographic basal gradient and **d** post-extrasystolic gradient correlated to the CMR scar tissue

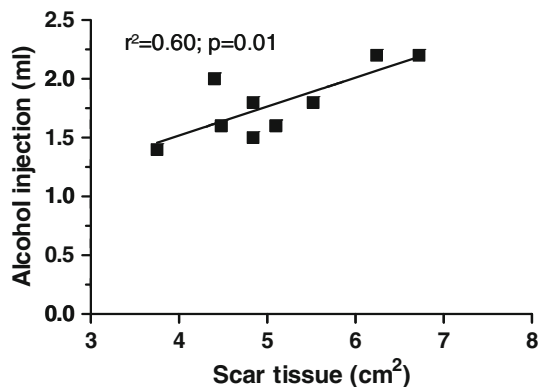
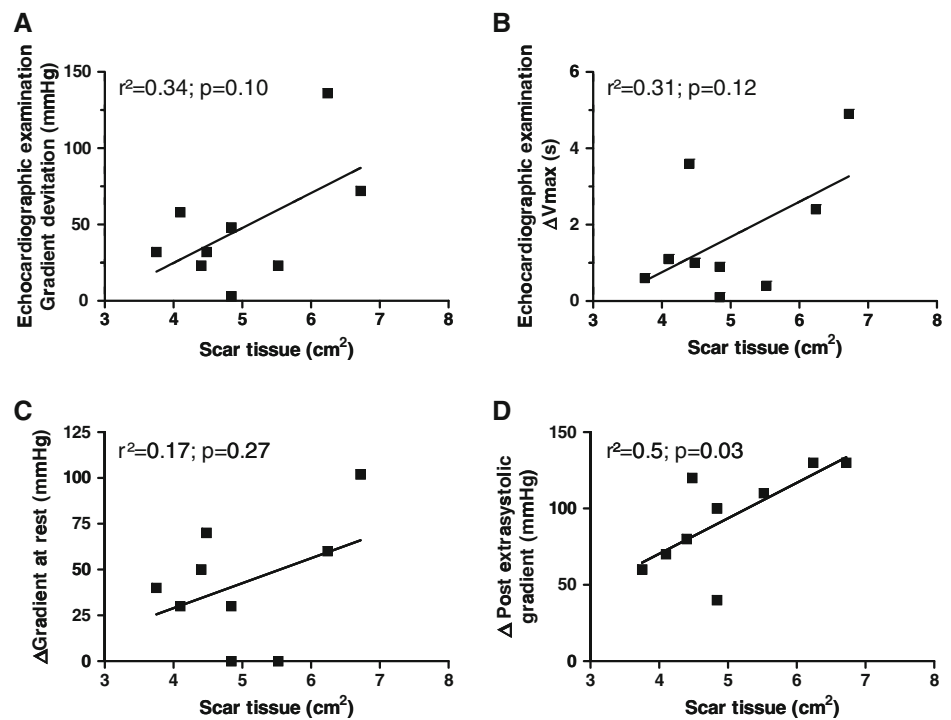


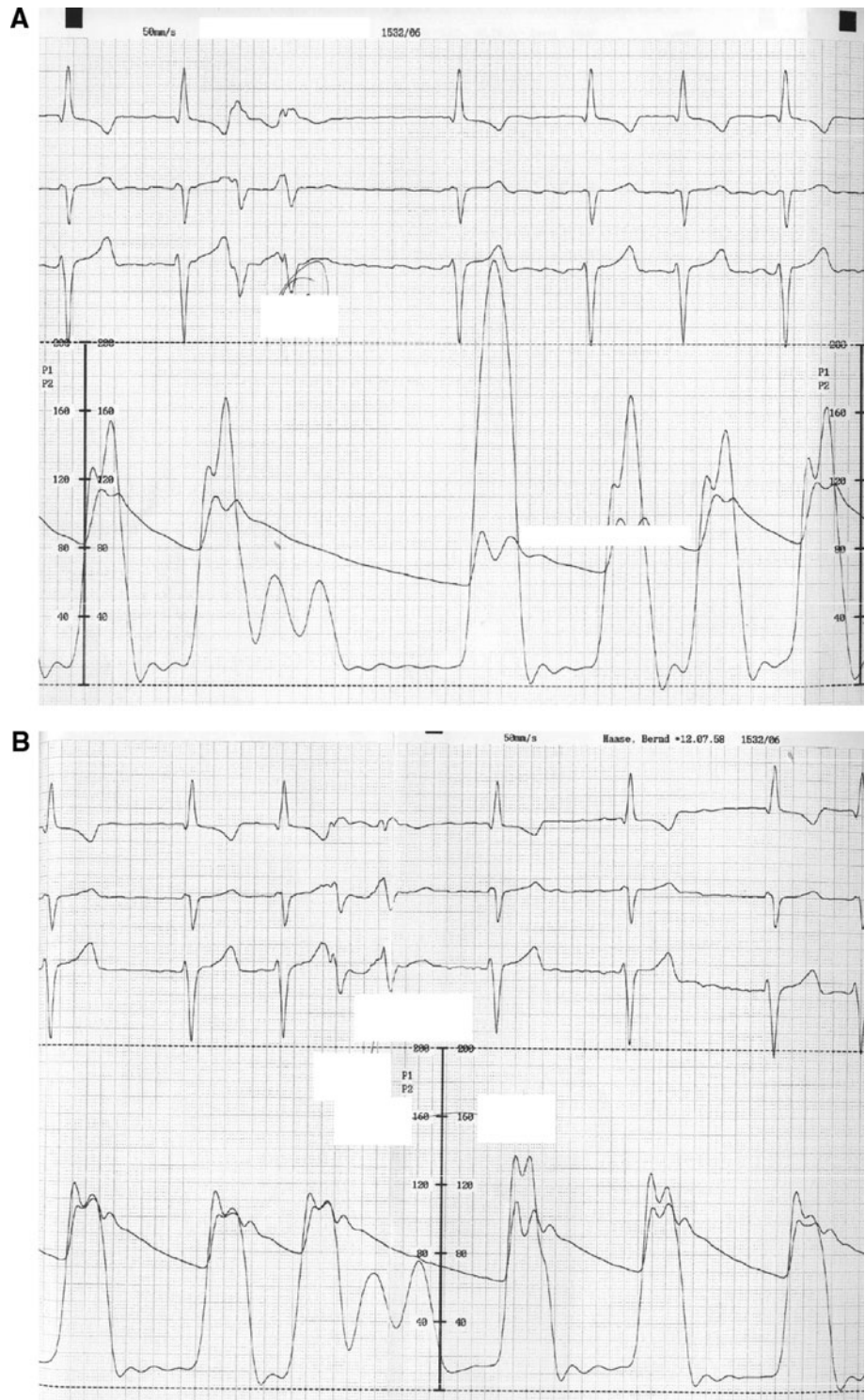
Fig. 3 Correlation between quantity of injected ethanol and the CMR scar tissue

referred to the procedure as percutaneous transluminal septal myocardial ablation (PTSMA), whereas Gietzen et al. [13, 27] have called the procedure transc coronary ablation of septal hypertrophy (TASH). There is enough evidence to show that the amount of ethanol used and the number of septal perforator arteries ablated determine the height of the creatine kinase (CK) rise, the degree of acute gradient reduction (Fig. 4) and the incidence of complete heart block and mortality [13, 17, 27, 31]. The introduction of myocardial contrast echocardiography by Faber et al. [16] allows for the correct identification of the appropriate septal perforator to be occluded and the avoidance of occluding septal perforators that supply distant areas of the myocardium such as the papillary muscles or the free wall

of the left or right ventricle. However, it has been shown that the amount of septum reduction increases further with time after TASH [32]. The observation that there is further gradient reduction in the year following the procedure has led to a less aggressive approach in terms of the amount of ethanol used and the number of vessels ablated during the procedure with a resulting decrease in the incidence of heart block [13, 17, 20, 27, 31, 32].

The TASH procedure is a promising nonsurgical technique for the reduction of symptoms and the LVOT gradient in HOCM. Several studies have shown clinical success rates with TASH application, varying from 90 to 100% [13, 15, 18, 20, 31, 32]. This is in line with our findings. Our results demonstrate a clinical success rate defined as a reduction of the echocardiographic LVOT gradient at rest, septum thickness, invasively assessed gradient at rest and gradient after stimulation of 100% (Fig. 1). The invasive measurements showed a significant decrease of the basal LVOT gradient at rest and also of the post-extrasystolic gradient after the TASH procedure (Figs. 1, 4). The echocardiographic examination of the LVOT gradient under basal conditions, the maximal flux acceleration over the aortic valve and septum size before and after TASH treatment confirms these results (Fig. 1). We could show a TASH-associated improvement in all examinations. Consequently, TASH was highly effective in improving hemodynamic and anatomic conditions. Furthermore, the TASH procedure has some advantages in comparison to myectomy surgery. These advantages include: the avoidance of cardiopulmonary bypass with

Fig. 4 A 50-year-old male patient with HOCM and TASH. **a** Angiography protocol before TASH showing a post-extrasystolic gradient at rest of 150 mmHg. **b** After the procedure the post-extrasystolic gradient is documented as maximal 40 mmHg

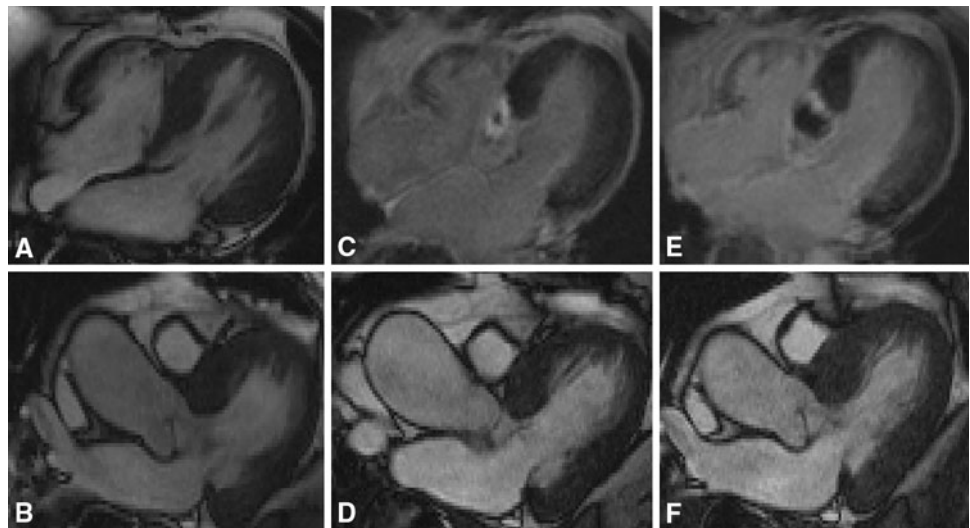


attendant risks, especially in elderly patients, as well as a shorter hospitalization period. Although two large German studies reported longer hospital residencies for supervision for delayed heart block [13, 31], a shorter recovery time and less expenses were recorded.

On the other hand, the advantages of myectomy surgery include: more immediate and complete relief of resting and

provoked obstruction and concomitant mitral regurgitation, as well as smaller incidences of complete heart block, requiring a pacemaker. There are excellent long-term results with no risk of coronary dissection or unwanted myocardial infarction. There is no evidence in long-term studies that myectomy is arrhythmogenic, has ability to deal with concomitant problems such as mid-ventricular

Fig. 5 An 82-year-old female patient with HOCM. MRI at four-chamber view (a, c, e) and at three-chamber view (b, d, f) before (a, b) and after TASH (c, d, e, f). a, c and e In each case late enhancement pictures after intravenous contrast medium injection. In the four-chamber view confirmation of scar tissue in the septum area (c, e). b, d and f in each case pictures in cine mode in the three-chamber view with SAM phenomenon which impresses slightly declining



obstruction, constricting muscle bridges over the left anterior descending coronary artery, and aortocoronary bypass surgery. It does not cause right ventricular outflow obstruction, mitral valve repair or replacement for additional valvular problems, and concerning a small but significant amount of patients, it is not able to carry out NSRT for technical reasons, and NSRT may be less effective in younger patients with thicker septum [33] and in other specific circumstances.

There is still a considerable debate on the optimal procedure in the management of subaortic obstructive HCM. On the one hand the ambition of TASH is the reduction of symptoms and the LVOT gradient in HOCM. On the other hand it is essential to reduce the collateral complications of the nonsurgical procedure like RBBB (in almost 50% of the patients) and high-grade atrioventricular block requiring permanent pacing in 10% [34]. Therefore, it is important to create a small-sized infarction-area. The role of CMR was to estimate the anatomical conditions before starting the intervention and to clarify the broadening of scar tissue. In our opinion, the current role and future potential of CMR in TASH has not been investigated sufficiently. It is accepted that CMR is the gold standard imaging tool to access cardiac masses or to measure cardiac scar tissue [35–39]. Furthermore, CMR has an outstanding role in ischemia diagnostic and coronary artery disease (CAD) [40–49]. To our knowledge this is the first study that shows a direct correlation of the CMR scar tissue and the effectiveness of TASH.

One aim of this study was to evaluate the ideal diagnostic imaging modality to illustrate the effectiveness of the TASH procedure. Another aim was to assess if the broadening of the infarction area correlates with the reduction of the LVOT gradient. After the successful TASH procedure the scar tissue was appraised by CMR and the infarction area was correlated with the decrease of the LVOT gradient the septum downsizing and the ethanol injection. Figure 2

shows a correlation between each examination and the corresponding scar tissue. There was no significant correlation between the echocardiographic investigations and the corresponding scar tissue into the CMR investigation. Consequently, echocardiography may not be able to visualize the effectiveness of TASH significantly. Concerning the invasive measurements, Fig. 2c also delivers a nonsignificant result for the correlation of the angiographic LVOT gradient at rest and the imaged infarction area. In Fig. 2d the post-extrasystolic gradient is plotted against the scar tissue. There was a statistical significant correlation between the different investigation methods ($P = 0.03$, $r^2 = 0.5$). Furthermore, our results suggest some answers in the remaining areas of uncertainty concerning the different effects of varying ethanol dosing within TASH. Veselka et al. [50], compared the effect of a “high dose” (2.8 ± 0.6 ml) versus a “low dose” (1.5 ± 0.4 ml) of ethanol, resulting in CK peaks of about six- versus ninefold above their upper reference value of 0.4 Kat/l. As the main conclusion, no difference was found with respect to hemodynamic efficiency during short-term follow-up in 42 patients. This is in concert with several other studies which suggest, that a correctly placed ablation lesion, releasing a CK peak of five- to nine-fold, should be high enough to substantially reduce or eliminate the LVOT obstruction during a 12-month local remodeling process [27, 51, 52]. In our study, the mean amount of ethanol injected was 1.8 ± 0.3 ml (Table 1). The results of our study show a significant correlation between the amount of injected ethanol and scar tissue investigated by CMR (Fig. 3, $P = 0.01$, $r^2 = 0.6$). Consequently, these data underline the outstanding importance of the correctly placed TASH procedure. Our analysis clarifies the ability of CMR to deliver a direct in vivo evaluation of the ethanol associated infarction area (Figs. 5, 6). Thus, it offers an independent alternative to laboratory testing and other imaging techniques.

Fig. 6 A 68-year-old female patient with HOCM. **a** septum nose before and **b** after the TASH procedure, with reduction of the *marked areas*

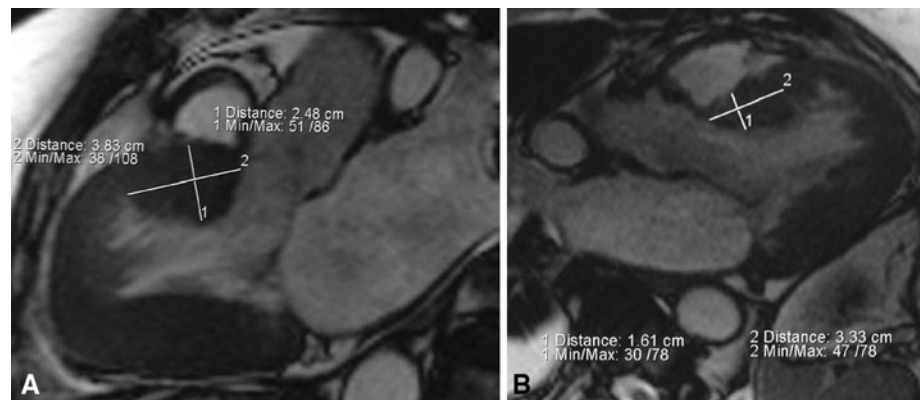
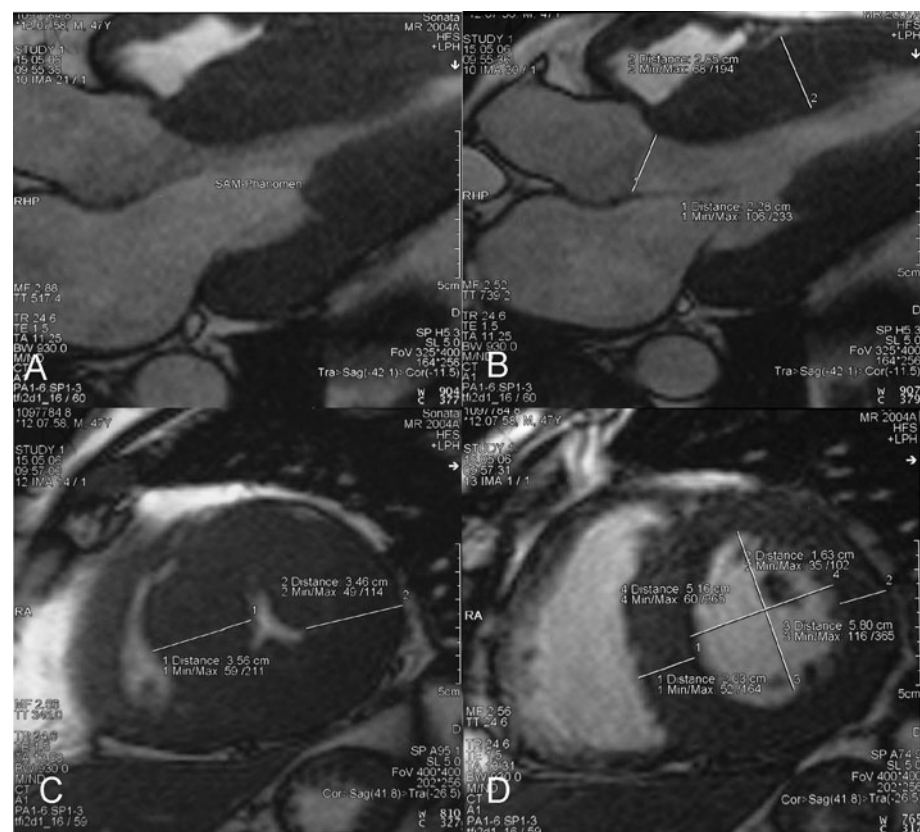


Fig. 7 A 78-year-old male patient with each MR investigation into cine mode before TASH. **a** SAM phenomenon, **b**, **c** and **d**. Measurement of dimensions, **b** at three-chamber view, **c** at short axis (*end-systolic*) and **d** at short axis (*end-diastolic*)



This indicates that a combined technique of invasive measurements and noninvasive CMR is ideally suited to assess the efficiency of TASH in ventricular hypertrophy and remodeling, which may allow a reduction in sample size to show clinically relevant effects. A comprehensive functional assessment is possible by CMR because of its capability to measure the flow velocity and the flow volume, which are the basic requirements to quantify lesion severity in a heart disease, which was formerly the main focus of echocardiography (Fig. 7) [35, 36, 40]. Another important advantage of CMR over other imaging methods that are used to assess myocardial viability is that it shows

the transmural extent of viable myocardium (Fig. 5) [41]. This leads to the possibility of visualizing the ethanol determined infarction area as scar tissue. Furthermore, major technical advances have considerably improved acquisition speed and image quality thus making CMR a useful tool for the evaluation of patients with ischemic heart disease [42–49].

Our study has several limitations. It has to be considered that there is only a relative small study population which leads to high range of individual variability. Probably, some results would have reached statistical significant correlation with a greater amount of patients. Patients were

not assigned randomly. Larger studies with more patients have to be conducted. The M-mode measurements of left atrial and left ventricular dimensions may not sample exactly maximum and minimum wall thickness, may be subject to angle errors, and were not performed blinded with respect to treatment status.

We come to the conclusion that CMR offers a potentially more accurate noninvasive technique for in vivo comparison of scar tissue than echocardiography. Furthermore, CMR provides images with high spatial resolution, free of geometric constraints, as well as precise volumetric quantification of abnormalities and direct anatomical correlation (Figs. 5, 6). We conclude that, the optimal modality to visualize the TASH effect seems to be a combination between CMR-imaging and the invasive identification of the post-extrasystolic gradient.

Acknowledgments Prof. Maier is funded by the Deutsche Forschungsgemeinschaft (DFG) through grants for a Clinical Research group (MA 1982/2-2) and by a DFG Heisenberg grant (MA 1982/4-1).

Open Access This article is distributed under the terms of the Creative Commons Attribution Noncommercial License which permits any noncommercial use, distribution, and reproduction in any medium, provided the original author(s) and source are credited.

References

1. Maron BJ, McKenna WJ, Danielson GK, Kappenberger LJ, Kuhn HJ, Seidman CE, Shah PM, Spencer WH, Spirito P, Ten Cate FJ, Wigle ED (2003) ACC/ESC clinical expert consensus document on hypertrophic cardiomyopathy: a report of the American College of Cardiology Task Force on Clinical Expert Consensus Documents and the European Society of Cardiology Committee for Practice Guidelines. *J Am Coll Cardiol* 42:1687–1713
2. Loogen F, Kuhn H, Gietzen F, Loesse B, Schulte HD, Bircks W (1983) Clinical course and prognosis of patients with typical and atypical hypertrophic obstructive and with hypertrophic nonobstructive cardiomyopathy. *Eur Heart J* 4:145–153
3. Maron BJ, Bonow RO, Cannon RO 3rd, Leon MB, Epstein SE (1987) Hypertrophic cardiomyopathy: interrelations of clinical manifestations, pathophysiology, and therapy (1). *N Engl J Med* 316:780–789
4. Wigle ED, Rakowski H, Kimball BP, Williams WG (1995) Hypertrophic cardiomyopathy: clinical spectrum and treatment. *Circulation* 92:1680–1692
5. Spirito P, Seidman CE, McKenna WJ, Maron BJ (1997) The management of hypertrophic cardiomyopathy. *N Engl J Med* 336:775–785
6. Morrow AG, Reitz BA, Epstein SE, Henry WL, Conkle DM, Itsoitz SB, Redwood DR (1975) Operative treatment in hypertrophic subaortic stenosis: techniques, and the results of pre and postoperative assessments in 83 patients. *Circulation* 52: 88–102
7. Maron BJ, Epstein SE, Morrow AG (1983) Symptomatic status and prognosis of patients after operation for hypertrophic obstructive cardiomyopathy: efficacy of ventricular septal myotomy and myectomy. *Eur Heart J* 4(suppl F):175–185
8. Schulte HD, Borisov K, Gams E, Gramsch-Zabel H, Loesse B, Schwartzkopff B (1999) Management of symptomatic hypertrophic obstructive cardiomyopathy: long-term results after surgical therapy. *Thorac Cardiovasc Surg* 47:213–218
9. Robbins RC, Stinson EB (1996) Long-term results of left ventricular myotomy and myectomy for obstructive hypertrophic cardiomyopathy. *J Thorac Cardiovasc Surg* 111:586–594
10. Maron BJ, Bonow RO, Cannon RO 3rd, Leon MB, Epstein SE (1987) Hypertrophic cardiomyopathy: interrelations of clinical manifestations, pathophysiology, and therapy (2). *N Engl J Med* 316:844–852
11. Kuhn H, Gietzen F, Ch Leuner, Gerenkamp T (1997) Induction of subaortic septal ischaemia to reduce obstruction in hypertrophic obstructive cardiomyopathy: studies to develop a new catheter-based concept of treatment. *Eur Heart J* 18:846–851
12. Sigwart U (1995) Non-surgical myocardial reduction for hypertrophic obstructive cardiomyopathy. *Lancet* 346:211–214
13. Gietzen FH, ChJ Leuner, Raute-Kreinsen U, Dellmann A, Heggemann J, Strunk-Mueller C, Kuhn HJ (1999) Acute and long-term results after transcatheter ablation of septal hypertrophy (TASH): catheter interventional treatment for hypertrophic obstructive cardiomyopathy. *Eur Heart J* 20:1342–1354
14. Kuhn H, Gietzen FH, Schäfers M, Freick M, Gockel B, Strunk-Müller C, Jachmann E, Schober O (1999) Changes in the left ventricular outflow tract after transcatheter ablation of septal hypertrophy (TASH) for hypertrophic obstructive cardiomyopathy as assessed by transoesophageal echocardiography and by measuring myocardial glucose utilization and perfusion. *Eur Heart J* 20:1808–1817
15. Knight C, Kurbaan AS, Seggewiss H, Henein M, Gunning M, Harrington D, Fassbender D, Gleichmann U, Ul Sigwart (1997) Nonsurgical septal reduction for hypertrophic obstructive cardiomyopathy: outcome in the first series of patients. *Circulation* 95:2075–2081
16. Faber L, Seggewiss H, Gleichmann U (1998) Percutaneous transluminal septal myocardial ablation in hypertrophic obstructive cardiomyopathy: results with respect to intraprocedural myocardial contrast echocardiography. *Circulation* 98:2415–2421
17. Lakkis NM, Nagueh SF, Kleimann NS, Killip D, He ZX, Verani MS, Roberts R, Spencer WH 3rd (1998) Echocardiography-guided ethanol septal reduction for hypertrophic obstructive cardiomyopathy. *Circulation* 98:1750–1755
18. Boekstegers P, Steinbigler P, Molnar A, Schwaiblmair M, Becker A, Knez A, Haberl R, Steinbeck G (2001) Pressure-guided non-surgical myocardial reduction induced by small septal infarctions in hypertrophic obstructive cardiomyopathy. *J Am Coll Cardiol* 38:846–853
19. Mazur W, Nagueh SF, Lakkis NM, Middleton KJ, Killip D, Roberts R, Spencer WH 3rd (2001) Regression of left ventricular hypertrophy after nonsurgical septal reduction therapy for hypertrophic obstructive cardiomyopathy. *Circulation* 103:1492–1496
20. Nagueh SF, Ommen SR, Lakkis NM, Killip D, Zoghbi WA, Schaff HV, Danielson GK, Quinones MA, Tajik AJ, Spencer WH (2001) Comparison of ethanol septal reduction therapy with surgical myectomy for the treatment of hypertrophic obstructive cardiomyopathy. *J Am Coll Cardiol* 38:1701–1706
21. Wigle ED, Schwartz L, Woo A, Rakowski H (2001) To ablate or operate? That is the question!. *J Am Coll Cardiol* 38:1707–1710
22. Fananapazir L, McAreavey D (1998) Therapeutic options in patients with obstructive hypertrophic cardiomyopathy and severe drug-refractory symptoms. *J Am Coll Cardiol* 31:259–264
23. Kuhn H, Gietzen FH, Leuner C, Schäfers M, Schober O, Strunk-Müller C, Obergassel L, Freick M, Gockel B, Lieder F, Raute-Kreinsen U (2000) Transcatheter ablation of septal hypertrophy

- (TASH): a new treatment option for hypertrophic obstructive cardiomyopathy. *Z Kardiol* 89(4):41–54
24. Spirito P, Maron BJ (1999) Perspectives on the role of new treatment strategies in hypertrophic obstructive cardiomyopathy. *J Am Coll Cardiol* 33:1071–1075
 25. Maron BJ (1999) New interventions for obstructive hypertrophic cardiomyopathy: promise and prudence. *Eur Heart J* 20:1292–1294
 26. Braunwald E (2002) Hypertrophic cardiomyopathy: the benefits of a multidisciplinary approach. *N Engl J Med* 347:1306–1307
 27. Kuhn H, Lawrenz Lieder F, Leuner C, Strunk-Müller C, Obergassel L, Bartelsmaer M, Stellbrink C (2008) Survival after transcatheter ablation of septal hypertrophy in hypertrophic obstructive cardiomyopathy (TASH): a 10 year experience. *Clin Res Cardiol* 97:234–243
 28. Sahn DJ, De Maria A, Kisslo J, Weymann A (1978) Recommendations regarding quantitation in M-mode echocardiography: results of a survey of echocardiographic measurements. *Circulation* 58:1072–1083
 29. Gilbert BW, Pollick C, Adelman AG, Wigle ED (1980) Hypertrophic cardiomyopathy: subclassification by M-mode echocardiography. *Am J Cardiol* 45:861–872
 30. Klues HG, Leuner C, Kuhn H (1992) Left ventricular outflow tract obstruction in patients with hypertrophic cardiomyopathy: increase in gradient after exercise. *J Am Coll Cardiol* 19:527–533
 31. Seggewiss H, Faber L, Gleichmann U (1999) Percutaneous transluminal septal ablation in hypertrophic obstruction cardiomyopathy. *Thorac Cardiovasc Surg* 47:94–100
 32. Alam M, Dokainish H, Lakkis N (2006) Alcohol septal ablation for hypertrophic obstructive cardiomyopathy: a systematic review of published studies. *J Interv Cardiol* 19:319–327
 33. Seggewiss H, Faber L, Ziemssen P (2000) Age related acute results of percutaneous septal ablation in hypertrophic obstructive cardiomyopathy (abstract). *J Am Coll Cardiol* 35(Suppl A):188A
 34. Sathyamurthy I (2006) Transcatheter ablation of septal hypertrophy (TASH). *Indian Heart J* 58:371–374
 35. Watzinger N, Maier R, Reiter U, Reiter G, Fuernau G, Wonisch M, Fruhwald FM, Schumacher M, Zweiker R, Rienmueller R, Klein W (2005) Clinical applications of cardiovascular magnetic resonance. *Curr Pharm Des* 11:457–475
 36. Bernhardt P, Engels T, Knuf B, Strohm O (2006) Cardiac magnetic resonance in outpatients in Germany—indications, complications and protocol suggestions from a high-volume center. *Int J Cardiol* 28(111):86–91
 37. Schroeder J, Peterschroeder A, Vaske B, Butz T, Barth P, Oldenburg O, Bitter T, Burchert W, Horstkotte D, Langer C (2009) Cardiac volumetry in patients with heart failure and reduced ejection fraction: a comparative study correlating multi-slice computed tomography and magnetic resonance tomography; reasons for intermodal disagreement. *Clin Res Cardiol* 98:739–747
 38. Pilz G, Bernhardt P, Harrer E, Klos M, Höfling B (2008) Cardiac magnetic resonance imaging: an essential diagnostic aid in suspected myocardial re-infarction in a 40 year old woman. *Clin Res Cardiol* 97:280–283
 39. Schwab J, Haack G, Sinns D, Bär I, Zahn R (2007) Diagnosis of left ventricular myxoma with cardiac magnetic resonance imaging. *Clin Res Cardiol* 96:189–190
 40. Altbach MI, Squire SW, Kudithipudi V, Castellano L, Sorrell VL (2007) Cardiac MRI is complementary to echocardiography in the assessment of cardiac masses. *Echocardiography* 24:286–300
 41. Kim RJ, Wu E, Rafael A, Chen EL, Parker MA, Simonetti O, Klocke FJ, Bonow RO, Judd RM (2000) The use of contrast-enhanced magnetic resonance imaging to identify reversible myocardial dysfunction. *N Engl J Med* 343:1445–1453
 42. Nandalur KR, Dwamena BA, Choudhri AF, Nandalur MR, Carlos RC (2007) Diagnostic performance of stress cardiac magnetic resonance imaging in the detection of coronary artery disease: a meta-analysis. *J Am Coll Cardiol* 50:1343–1353
 43. Baer FM, Thiessen P, Schneider CA, Voth E, Sechtem U, Schichta H (1998) Dobutamine magnetic resonance imaging predicts contractile recovery of chronically dysfunctional myocardium after successful revascularisation. *J Am Coll Cardiol* 31:1040–1048
 44. Wellhofer E, Olariu A, Klein C, Grafe M, Wahl A, Fleck E, Nagel E (2004) Magnetic resonance low-dose dobutamine test is superior to SCAR quantification for the prediction of functional recovery. *Circulation* 109:2172–2174
 45. Gotte MJ, van Rossum AC, Twisk JWR, Kuijper JPA, Marcus JT, Visser CA (2001) Quantification of regional contractile function after infarction: strain analysis superior to wall thickening analysis in discriminating infarct from remote myocardium. *J Am Coll Cardiol* 37:808–817
 46. Plein S, Kozerke S, Suder D, Luescher TF, Greenwood JP, Boesiger P, Schwittler J (2008) High spatial resolution myocardial perfusion cardiac magnetic resonance for the detection of coronary artery disease. *Eur Heart J* (Epub ahead of print)
 47. Merkle N, Wöhrle J, Nusser T, Grebe O, Spiess J, Torzewski J, Hombach V (2009) Diagnostic performance of magnetic resonance first pass perfusion imaging is equally potent in female compared to male patients with coronary artery disease. *Clin Res Cardiol*, Sep 11 (Epub ahead of print)
 48. Jensen CJ, Bleckmann D, Eberle HC, Nassenstein K, Schlosser T, Sabin GV, Naber CK, Bruder O (2009) A simple MR algorithm for estimation of myocardial salvage following acute ST segment elevation myocardial infarction. *Clin Res Cardiol* 98:651–656
 49. Doesch C, Seeger A, Hoewelborn T, Klumpp B, Fenchel M, Kramer U, Schönfish B, Claussen CD, Gawaz M, Miller S, May AE (2008) Adenosine stress cardiac magnetic resonance imaging for the assessment of ischemic heart disease. *Clin Res Cardiol* 97:905–912
 50. Veselka J, Duchonová R, Procházková S, Pálenícková J, Sorajja P, Tesar D (2005) Effects of varying ethanol dosing in percutaneous septal ablation for obstructive hypertrophic cardiomyopathy on early hemodynamic changes. *Am J Cardiol* 95:675–678
 51. Faber L, Welge D, Fassbender D, Schmidt HK, Horstkotte D, Seggewiss H (2007) One-year follow-up of percutaneous septal ablation for symptomatic hypertrophic obstructive cardiomyopathy in 312 patients: predictors of hemodynamic and clinical response. *Clin Res Cardiol* 96:864–873
 52. Lawrenz T, Lieder F, Leuner CJ, Obergassel L, Gockel B, Strunk-Mueller C, Kuhn H (2003) What is the correct amount of ethanol in the catheter based treatment for hypertrophic obstructive cardiomyopathy? *Eur Heart J* 24(Suppl):136